



Functional interplay between p53 and $\Delta 133p53$ in adaptive stress response

Lu Gong^{1,2} · Xiao Pan³ · Gamze K. Abali^{1,2} · John B. Little² · Zhi-Min Yuan^{1,2}

Received: 25 March 2019 / Revised: 10 October 2019 / Accepted: 15 October 2019 / Published online: 28 October 2019
© The Author(s), under exclusive licence to ADMC Associazione Differenziamento e Morte Cellulare 2019

Abstract

Apart from its well-known prodeath activity, p53 is also implicated in promoting cell survival. How p53 can mediate such seemingly opposing effects is largely unclear. We report here a novel mechanism in which p53-mediated proapoptosis is switched to antiapoptosis via its interaction with a p53 isoform, $\Delta 133p53$. We show that the expression of $\Delta 133p53$ is induced by mild or a moderate level of stress via an HIF1-dependent mechanism. Increased $\Delta 133p53$ levels contribute to the adaptive response by shifting the p53 binding at the *Bcl2* promoter from suppressive responsive elements (RE) to activating REs, resulting in induction of *Bcl2*. In accordance with this mode of action, pretreatment of mice with mild stress induces $\Delta 133p53$ and *Bcl2*, which is associated with protection of animals from toxicity caused by high doses of DNA damage agents. Collectively, our work uncovers a novel functional interplay between p53 and $\Delta 133p53$ determining cell fate; survival or death in response to stress.

Introduction

As a protein critical for the maintenance of homeostasis, p53 induces apoptosis or senescence in response to severe stress to protect organismal fidelity by eliminating irreparably damaged cells. However, evidence indicates that p53 can also promote adaptation and survival response to mild stress supporting organismal fitness [1]. It is unclear how p53 can mediate such opposing prosurvival and prodeath activities. Available information indicates that p53, as a

multifunctional protein, serves as a hub that interfaces with a variety of proteins and pathways to regulate cellular responses either positively or negatively. Among a host of proteins, p53 isoforms have been reported to intimately interact with p53 and to modulate p53 response to stress in a context dependent and isoform specific manner [2–4].

The mRNA of p53 isoforms is transcribed from the p53 gene by diverse mRNA splicing or driving by alternative promoters [2, 4]. Thirteen p53 isoforms have been identified hitherto [3]. Among them, $\Delta 133p53$ is relatively well characterized because of its unique expression pattern and function relative to full-length p53. We previously reported that in human cells, $\Delta 133p53$ can induce *RAD51*, *RAD52*, and *LigaseIV* expression in a p53 independent fashion to promote DNA double strand break repair [5]. While this DNA repair function is shared by the zebrafish ortholog of $\Delta 113p53$, its mouse ortholog has yet to be discovered, preventing the use of murine models for functional characterization of $\Delta 133p53$.

We report here the identification of the $\Delta 133p53$ mouse ortholog—ME- $\Delta 123p53$. We show that ME- $\Delta 123p53$ is induced by moderate stress via an ROS-mediated mechanism. Increased ME- $\Delta 123p53$ expression is associated with enhanced cellular resistance to acute stresses including DNA damage and ribosomal stress. Mechanistically, ME- $\Delta 123p53$ binds to p53 resulting in a shift of the p53 binding from the repressive to activating element within the *Bcl2* promoter. Our data supports a model in which, moderate

These authors contributed equally: Lu Gong, Xiao Pan

Edited by X. Lu

Supplementary information The online version of this article (<https://doi.org/10.1038/s41418-019-0445-z>) contains supplementary material, which is available to authorized users.

✉ Zhi-Min Yuan
zyuan@hsph.harvard.edu

¹ Department of Environmental Health, Harvard T.H. Chan School of Public Health, Boston, MA 02115, USA

² John B. Little Center for Radiation Sciences, Harvard T.H. Chan School of Public Health, Boston, MA 02215, USA

³ First Affiliated Hospital and Institute of Translational Medicine, School of Medicine, Zhejiang University, Hangzhou 310006, China

stress induces alteration of ME- $\Delta 123p53$ /p53 ratio that determines cell survival or death in response to stresses.

Materials and methods

Cell culture

Mouse MEF, 3T3 cells, human GM-8680 fibroblasts, and 293T cells were cultured in DMEM (Hyclone, Chicago, IL), human H1299 cells were cultured in RPMI-1640 (Gibco, Waltham, MA). MEF cells were derived from C57BL mice, isolated from E14 embryos as previously described [6], then amplified for three passages for further usage. All other cells are from our lab stocks or purchased from American Type Culture Collection (ATCC, Manassas, VA). Cell lines have recently been tested for mycoplasma contamination. All medium was supplied with 10% fetal bovine serum (FBS, Gibco), 100 U/ml penicillin G and 100 μ g/ml streptomycin (Corning Cellgro, Corning, NY). All cells were cultured in cell incubators (Thermo Fisher, Waltham, MA) set 37 °C, 5% CO₂. Cells were passaged with 0.25% Trypsin solution (Thermo Fisher) digestion, fresh medium (containing 10% FBS) neutralizing and PBS washing.

Antibodies

For western blot, anti-mouse-p53 (F-8, Santa cruz, Santa Cruz, CA, sc-374087, 1:1000, for p53 and ME- $\Delta 123p53$), anti-human-p53 antibody DO-1 (Santa Cruz, sc-126, 1:2000), anti-human-p53 (for isoforms) antibody DO-11 (GeneTex, Irvine, CA, GTX5258, 1:1000), anti-mouse/human-p53 antibody Ab-1 (Millipore, Burlington, MA, OP03, 1:500), anti-hif1 α (Novusbio, Centennial, CO, NB100-479, 1:1000), anti-sod1 (Abcam, Cambridge, MA, ab16831, 1:1000), anti-bcl2 (Santa cruz, sc-7382, 1:1000), anti-cleaved caspase3 (Cell Signaling, Danvers, MA, #9664, 1:1000), anti-parp (Cell Signaling, #9532, 1:1000), and anti- β -actin antibody (Sigma, AC-15, 1:2000) was used.

RACE

5'RACE and 3'RACE of mouse *TRP53* and isoform was performed using the RLM-RACE kit (RNA Ligase Mediated Rapid Amplification of cDNA Ends, Ambion, Waltham, MA) according to the protocol provided by the manufacturer. Primers used were listed in Table S1.

RNA-Seq and ChIP-Seq datasets analysis

The raw reads of the RNA-Seq datasets from the study GSE100961, ChIP-Seq dataset from GSE61247 were dumped from NCBI Sequence Read Archive repository. For RNA-Seq

data, the reads from three replications of the control group (GSM2698076, GSM2698082, GSM2698088) and irradiation group (6 h post 6 Gy ionizing radiation, GSM2698080, GSM2698086, GSM2698092) were combined, respectively. Short read sequences were aligned to the mouse genome (mm9) with STAR 2.6.0. For ChIP-Seq dataset GSM1500749 (Input) and GSM1500751 (HIF1A immunoprecipitation), data were reanalyzed with Bowtie 2.3.4 and MACS2 2.1.1. The read coverage histogram with gene structure diagrams are generated with Integrative Genomics Viewer 2.4 (Broad Institute, Cambridge, MA).

Annexin V/7-AAD dual staining and FACS

To detect apoptosis and necrosis, the fixed cells were stained with Annexin V and 7-AAD (Annexin V-PE/7-AAD Apoptosis Detection Kit, eBioscience, Waltham, MA) as per the manufacturer's instructions and subsequently subjected to FACS cytometry using an FACS Calibur Flow Cytometer (BD Biosciences, Franklin Lakes, NJ). A minimum of 105 cells per sample were analyzed. The raw data were analyzed with Flowjo 7.6 and Microsoft Excel 2007 was used for the statistical analyses.

TUNEL assay

Cryosections of mice thymus and spleen were fixed with 4% PFA for 15 min, washed with PBS, and incubated in permeabilization solution (0.1% Triton X-100, 0.1% sodium citrate) for 5 min on ice. Then TUNEL assay was carried out with the In Situ Cell Death Detection Kit, Fluorescein (Roche, Basel, Switzerland, 11684795910).

siRNA-based gene knockdown

siRNA target mouse *ME- $\Delta 123p53$* 5'UTR region and start codon region, siRNA target mouse *Bcl2* were synthesized by Sigma (St Louis, MO). The sequences of these siRNA were as follows: ME- $\Delta 123p53$ (ATG) siRNA (as ME- $\Delta 123p53$ i aforementioned), 5'-CAG CCU GAG CAU GGA AUA C-3'; ME- $\Delta 123p53$ (UTR) siRNA, 5'-CAG UUG AGG CAG GAU UGC U-3'; Bcl2 siRNA, 5'-GUA CAU ACA UUA UAA GCT G-3'. The plasmid pCAG/U6-HIF1 α i for HIF1 α knocking-down was purchased from Addgene.

For siRNA transfection, 1.0×10^5 cells in six-well plates were transfected with a mixture of siRNA and Lipofectamine 2000 (Invitrogen, Waltham, MA) according to manufacturer's instruction.

Plasmid cloning and mutation

Open reading frame (ORF) of p53 and ME- $\Delta 123p53$ were amplified with primers listed in Tabel S2 from genomic

DNA. Then p53 and ME- Δ 123p53 ORF were cloned into pCS2+ backbone (from RZPD, Berlin, Germany) as described previously [5]. ME- Δ 87p53 and ME- Δ 123p53 (Δ OD) were further generated based on ME- Δ 123p53 plasmid.

ME- Δ 123p53 mutations on p53 DNA-binding domain (DBD) R172H and R270H were generated from CMV-ME- Δ 123p53 plasmid with Q5 site-directed mutagenesis kit (New England Biolabs, Ipswich, MA). Mutation primers were listed in Table S2. Mutation PCR amplicons were treated with kinase-ligase-Dpn1 enzyme. All procedures were performed as manufacturer's instruction.

Preparation of adenovirus

For generating ME- Δ 123p53 expressing adenovirus plasmid (Ad-ME- Δ 123p53), full coding sequence of ME- Δ 123p53 was cloned into pAdTrack-CMV vector (a gift from Bert Vogelstein, Addgene plasmid #16405) [7], then recombined with pAdeasy-1 (Agilent Technologies, Santa Clara, CA, #240005) adenoviral backbone in BJ5183 competent cells as manual described. Positive colonies were identified by sequencing. Adenovirus were generated as manufacturer's instruction, and purified with Adeno-X Maxi Purification Kit (Takara, Kyoto, Japan, 631532). The titre of adenovirus was determined by titration in HEK293 cells.

For ME- Δ 123p53 shRNA expressing adenovirus plasmid (Ad-ME- Δ 123p53sh), shRNA was designed targeting to ME- Δ 123p53 unique 5'UTR and start codon (5'-AAGGCCAGCCTGAGCATGGAA-3') and cloned into pLKO.1 vector. The hU6 promoter, ME- Δ 123p53 shRNA, and terminator were amplified and subcloned into pShuttle vector. The following procedure was as Ad-ME- Δ 123p53.

The adenovirus expressing mouse Mir-364-3p was purchased from Abmgood (AdmiRa-mmu-miR-364-3p Virus, mm1357).

For introducing adenovirus in vivo, about 6×10^9 pfu adenovirus (diluted in 100 μ l PBS) was intraperitoneally injected into mice.

Luciferase reporters assay

About 3 kb promoters of ME- Δ 123p53, *Bcl2* or different fragments were amplified from MEF cells genomic DNA, and cloned into pGL3 luciferase reporter vectors respectively. Reporters with mutated p53/ME- Δ 123p53 response elements (REs) were generated with Q5 site-directed mutagenesis kit (New England Biolabs) as manufacturer's instruction. All primers used for cloning and mutation were listed in Table S2.

MCF-7 cells were cultured in 48-well plates, and transfected with siRNA or plasmids as indicated. One hundred

nanograms of specified luciferase reporter plasmids and 10 ng Renilla reporter plasmids (as control) were also transfected simultaneously. After 24 h, the Firefly (from pGL3 reporters) and Renilla luciferase activity was measured with the Dual-luciferase reporter assay system (Promega, Fitchburg, WI) according to product instructions. The relative activity of promoters was derived from the ratio of Firefly luciferase/Renilla luciferase.

Chromatin immunoprecipitation (ChIP)

ChIP assay was performed as previously described [5]. To immunoprecipitate ectopically expressed HA tagged p53 and Myc tagged ME- Δ 123p53, about 1×10^7 MEFs were transfected with CMV-HA-p53, CMV-Myc-ME- Δ 123p53, their combination or empty vectors as control. After 12 h, cells were collected, fixed, and sonicated. After precleared, DNA/Protein complex were immunoprecipitated with anti-HA agarose resin (Thermo Fisher, 20181), anti-c-Myc agarose resin (Thermo Fisher, 20168) or recombinant protein G agarose (Thermo Fisher, 15920). After reverse cross-linking, proteins were digested by proteinase K (Fermentas, Waltham, MA), and DNA was purified with QIAquick PCR purification kit (Qiagen, Venlo, Netherlands). Purified DNA fragments were amplified by real-time qPCR and SsoAdvanced Universal SYBR Green Supermix (BioRad, Hercules, CA, 172-5270). Primers used in ChIP were listed in Table S1.

Real-time quantitative PCR (qRT-PCR)

Total RNA was extracted with TRIzol reagents (Invitrogen) as product manual described. Then, 1 μ g of total RNA was reverse transcribed with iScript cDNA synthesis kit (BioRad). Real-time quantitative PCR was performed with synthesized cDNA, primers and SsoAdvanced Universal SYBR Green Supermix (BioRad, 172-5270) according to manufacturer's instruction. All primers used for qRT-PCR were listed in Table S1.

Western blot and immunoprecipitation

For western blot, cells were lysed in buffer (50 mM Tris pH = 8.0, 150 mM NaCl, 1% SDS). Protein concentrations of the lysates were determined by BCA assay. Then the lysates were resolved by SDS-PAGE and immunoblotted with indicated antibodies as previously described.

For immunoprecipitation, cells were lysed in Pierce IP buffer (Thermo Fisher, #87787) with shivering by a 1 ml syringe (with 0.6 mm pin), then incubated with Pierce Anti-HA Agarose Beads (Thermo Fisher, #26181) or Anti-c-Myc Agarose Beads (Thermo Fisher, #20168) at 4°C overnight. Precipitated proteins were detected with Anti-c-Myc-Tag

antibody (Cell Signaling, #2278) or Anti-HA-Tag antibody (Cell Signaling, #3724).

Animal experiments

C57BL mice (5–6 weeks old) were bred in animal facility of Harvard School of Public Health. Mice were housed under pathogen-free conditions and maintained in a 12-h light/12-h dark cycle, with food and water supplied ad libitum. Mice were randomly divided into three groups with equal amount of males and females, and each group contained at least 12 mice. One group of mice was treated with 0.1 Gy X-ray once per day. One group was intraperitoneally injected with low-dose arsenic (LDA) (0.4 mg/kg arsenic, in 100 μ l PBS) every day. The control group was intraperitoneally injected with 100 μ l PBS every day. After 5 consecutive days of treatment, mice were subjected with 8 Gy X-ray treatment for survival test. For TUNEL assay or checking genes expression, mice were irradiated with 4 Gy X-ray. At 12 h post irradiation, mice were sacrificed, and tissue samples were collected. For ActD stimulation test, 60 μ g/kg ActD was injected intraperitoneally into mice instead of irradiation treatment. For data recording and analysis, the investigators were blinded to the experimental group setting.

All animal procedures were conducted in accordance with the Guidelines for the Care and Use of Laboratory Animals and were approved by the Institutional Animal Care and Use Committee at the Harvard School of Public Health.

Statistical analysis

Experiments with cell lines were repeated at least three times. All animal experiments have been repeated for 2–3 times and confirmed. Comparisons within a given assay were done by one-way repeated measures ANOVA. Comparisons between assays were done by two-way repeated measures ANOVA. Data points were determined by the mean of repeats and plotted with standard variation error bars.

Results

The identification of a novel p53 isoform ME- $\Delta 123p53$ in mice

We previously reported that human $\Delta 133p53$ and its zebrafish ortholog $\Delta 113p53$ could be induced by ionizing irradiation [5]. To search for the murine ortholog, we examined X-ray irradiated MEFs. A p53 isoform with a shortened 5' terminal mRNA was induced by X-ray treatment and detected by RACE (Fig S1A). Its protein product

had a size around 35 kDa and was recognized by an antibody against the C-terminal of p53 (Fig S1B). The result from sequencing revealed that the 5'UTR and the coding sequences of the first two amino acids of this p53 isoform were in an alternative exon, which was located in intron 4 of the *p53* gene (Fig. 1a). This new isoform was also found in published RNA-seq datasets [8] (Fig S1C). Similar to its ortholog $\Delta 133p53$ and $\Delta 113p53$, this mouse p53 isoform lacks all transcription activity domain (TAD) and part of the DBD (Figs. 1a, S1D). This p53 isoform is distinct from previous reported $\Delta 122p53$, which is not naturally expressed but designed to match human $\Delta 133p53$ for investigation its function in mice [9, 10]. It begins with its unique N-terminal "ME" (Methionine–Glutamic acid) following by the remaining part of p53 (123–390), thus we named it as ME- $\Delta 123p53$.

Mild stress induces ME- $\Delta 123p53$, which enhances cellular stress resistance

Ionization radiation is known to induce cellular response via, at least in part, production of ROS [11]. We thus tested whether other agents known to induce ROS could also affect the expression of ME- $\Delta 123p53$. Interestingly, treatment of MEFs or 3T3 cells with increasing doses of arsenic revealed that the expression of ME- $\Delta 123p53$ was induced by only low doses but not high doses of arsenic (Figs. 1b, c, S2A). A similar observation was made with other ROS-inducing chemicals including H_2O_2 , vitamin K3, and $K_2Cr_2O_7$. Induction of ME- $\Delta 123p53$ by all three chemicals was limited to the low-dose range (Fig S2B). We further verified LDA-induced ME- $\Delta 123p53$ expression by either knocking down or overexpressing ME- $\Delta 123p53$ (Fig S2C, D). Our data collectively showed that contrary to full-length p53, which was mainly induced by high levels of stress, ME- $\Delta 123p53$ was preferentially induced by a low level of stress. To corroborate this finding, we measured the ratio of p53 over ME- $\Delta 123p53$ at the transcription level and found that treatment of cells with a low level of arsenic or VK3 resulted in an increase in the mRNA level of ME- $\Delta 123p53$ but not p53.

The preferential induction of ME- $\Delta 123p53$ by low but not high doses of ROS-inducing chemicals, prompted us to investigate the stress adaptive response, i.e., mild stress induces resistance to toxicity caused by subsequent severe stress. We previously reported that pretreatment of cells with LDA induced resistance to radiation [11]. Consistent with the low-dose specific effects, pretreatment with low dose but not high doses of arsenic attenuated high-dose radiation (HDR)-induced cell killing (Figs. 1d, S2E, F). We extended our study on the adaptive response to other types of stresses including ribosomal stress inducer actinomycin D (ActD, 5 nM), low dose 5-fluorouracil (5-FU, 50 μ M), or

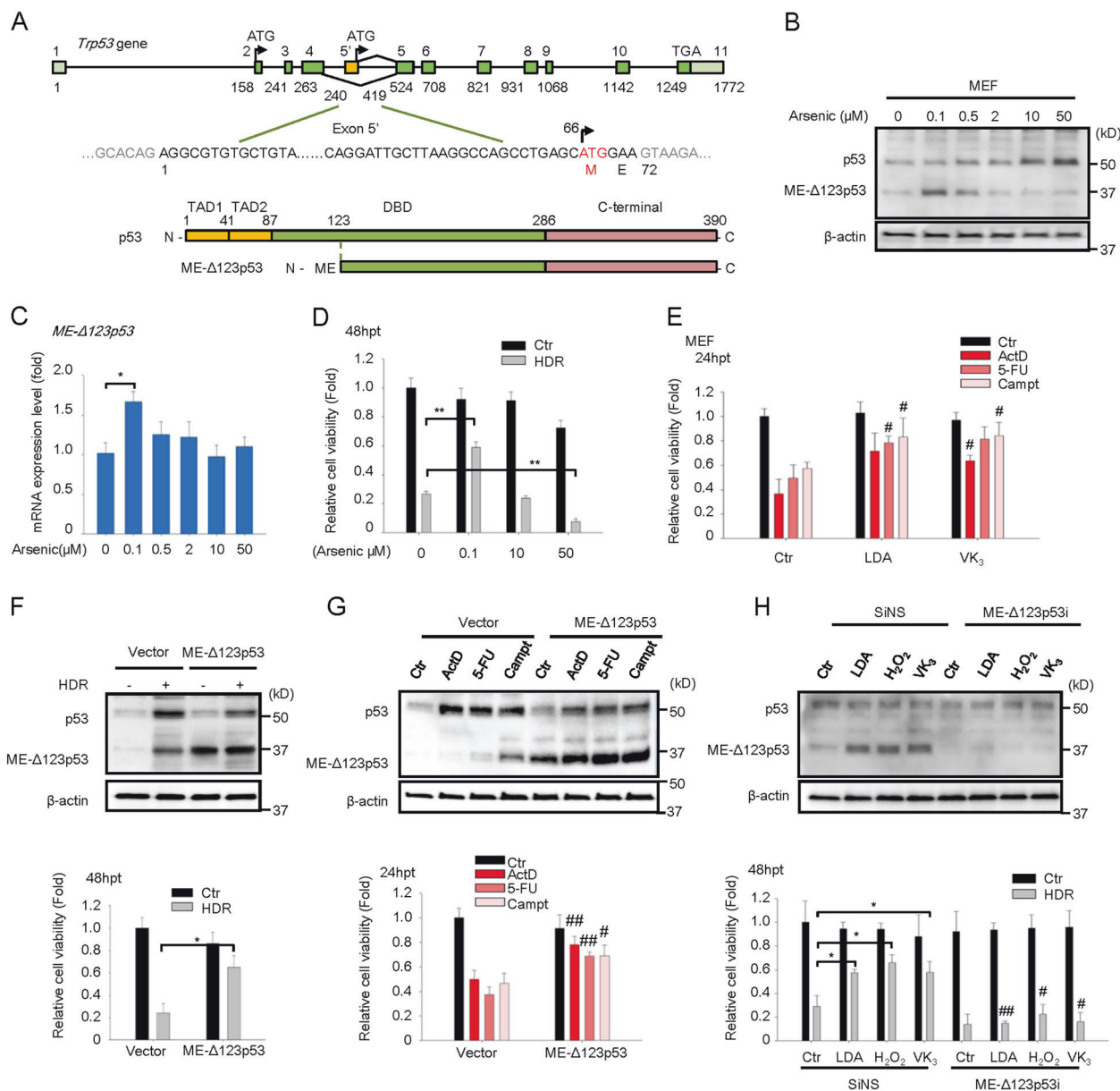


Fig. 1 Moderate stimulation induced a novel p53 isoform ME-Δ123p53 enhances cell resistance to acute stresses. **a** Mouse *Trp53* gene structure was shown in the diagram. *Trp53* gene has 11 exons and 10 introns, and each exon relative position is labeled. The start codon ATG of full-length p53 is located in exon 2. An alternative exon 5' in intron 4 contains 5'UTR and the coding sequence for the first two amino acids for a novel p53 isoform—ME-Δ123p53. ME-Δ123p53 lacks all transcription activity domain (TAD) and part of DNA-binding domain (DBD). Except the first two amino acids, the following parts are the same as full-length p53 from the 123th amino acid as shown. **b** MEF cells were pretreated with different doses of arsenic for 12 h, then p53 and ME-Δ123p53 protein abundance was determined by immunoblot, and **c** *ME-Δ123p53* mRNA level was measured by qRT-PCR. **d** MEF cells were pretreated with 0.1, 10, or 50 μM arsenic for 12 h, and then received 10 Gy X-ray high-dose irradiation (HDR). After 48 h of irradiation (hpt), relative cell viability was measured by trypan blue staining and counting. **e** MEF cells were pretreated with 0.1 μM arsenic or 0.5 μM VK₃ for 12 h, and then subjected with 5 nM actinomycin D (ActD), 50 μM 5-fluorouracil (5-FU) or 0.5 μM

Camptothecin (Campt) treatment. After 24 h of treatment (hpt), cell viability was measured. **f** MEFs were transfected with expression plasmids containing ME-Δ123p53 or empty vector, then subjected with HDR at 12 h after transfection. 48hpt, (top) p53 and ME-Δ123p53 protein level and (bottom) relative cell viability was measured. **g** MEF cells were transfected with ME-Δ123p53 plasmids or empty vector, and then treated with 5 nM ActD, 50 μM 5-FU, or 0.5 μM Campt at 12 h post transfection, (top) p53 and ME-Δ123p53 protein induction was measured by immunoblot. (Bottom) Cell viability was measured at 24hpt. **h** MEFs were transfected with siRNA targeting ME-Δ123p53 (ME-Δ123p53i) or nonsense siRNA (siNS), and then treated with 0.1 μM low dose arsenic (LDA), 50 μM H₂O₂, or 0.5 μM vitamin K₃ (VK₃) at 12 h post transfection. (Top) p53 and ME-Δ123p53 protein level was measured. After 12 h, cells were treated with HDR, and (bottom) relative cell viability was measured. Error bars denote standard deviation (**P* < 0.05, ***P* < 0.01). For comparing with the corresponding control sample, “#” was used instead of “*” for indicating *P* value range

DNA damage agent camptothecin (Campt, 0.5 μM) treatments. The result from cell survival experiments showed that LDA or low dose VK_3 pretreated MEFs exhibited significantly increased resistance to ribosomal stress and DNA damage (Figs. 1e, S2G, H).

To determine whether the observed protection was mediated by ME- $\Delta 123p53$, we either ectopically expressed or knocked down this p53 isoform. When compared with the vector control, expression of ME- $\Delta 123p53$ in MEFs was associated with a significant increase in cellular resistance to ribosomal stress or HDR-induced killing (Fig. 1f–g). Knocking down the expression of ME- $\Delta 123p53$ (ME- $\Delta 123p53i$) abrogated the resistance induced by LDA, H_2O_2 , and VK_3 resulting in enhanced HDR-induced cell killing (Fig. 1h). The data collectively indicate that treatment of cells with low doses of arsenic, H_2O_2 , or Vitamin K induced the expression of ME- $\Delta 123p53$, which resulted in increased cellular resistance to cell killing caused by DNA damage and ribosomal stress.

The chemicals tested here are commonly used ROS-producing agents, which elicit cellular response by inducing the production of ROS, particularly at the low-dose range. We thus directly tested whether ME- $\Delta 123p53$ induced by these chemicals was mediated by ROS. Treatment of cells with N-acetyl cysteine (NAC), a reducing agent, diminished ME- $\Delta 123p53$ induction by the chemicals, which was associated with loss of the protective effect against HDR-induced cells (Fig. 2a). The observation was corroborated by expressing super oxide dismutase 1 (SOD1), which inhibits ROS production. Similar to the use of NAC, SOD1 expression blunted the protection induced by the chemicals (Fig. 2b). The results together indicate that mild stress elicited by low levels of chemicals induces the expression of ME- $\Delta 123p53$ in ROS-dependent manner.

Our data revealed that ME- $\Delta 123p53$ expression is induced selectively by low levels of stress that promotes survival whereas p53 is induced by severe stress that causes cell death. We tested whether the distinct cell fate could be determined by different ratio of p53/ME- $\Delta 123p53$ (Fig. 2c). Increased expression of p53 was associated with decreased cell viability, as expected. ME- $\Delta 123p53$, when expressed alone, did not significantly affect cell viability however, when co-expressed with p53 it antagonized p53-dependent cell death in a dose-dependent manner (Fig. 2c). The effect of ME- $\Delta 123p53$ on cell viability was completely lost in $p53^{KO}$ MEFs (Fig S3A, B), establishing a p53-dependency. This result suggests that the relative cellular level of ME- $\Delta 123p53$ and p53 determines cell survival or death. We further confirmed the observation by expressing different levels of human p53 and $\Delta 133p53$ in human p53-null H1299 cells. Consistent with the result in MEFs, a higher ratio of $\Delta 133p53/p53$ was associated with

a greater resistance to HDR and Act. D-induced cell killing (Fig. 2d–f).

ME- $\Delta 123p53$ induction is mediated by ROS-induced HIF1

We went on probing the mechanism behind ROS-induced expression of ME- $\Delta 123p53$. Consistent with our previous finding that LDA induces HIF1 in an ROS-dependent fashion [11], immunoblot detected an elevated HIF1 α protein level in MEFs treated with LDA or low dose VK_3 (Fig. 3a, b). We next investigated whether HIF1 could mediate LDA-induced expression of ME- $\Delta 123p53$ by knocking down the expression of HIF1 (Figs. 3a, S3C). When compared with the control, U6-HIF1siRNA-mediated reduction of HIF1 expression impeded LDA-induced ME- $\Delta 123p53$ expression, resulting in loss of LDA-induced resistance to HDR. Overexpressing ME- $\Delta 123p53$ restored resistance (Fig S3D). The importance of HIF pathway in ME- $\Delta 123p53$ induction was also evident with low dose of VK_3 treatment (Fig. 3b).

To explore the molecular mechanism behind HIF1-dependent regulation of ME- $\Delta 123p53$ expression, we cloned its promoter from intron 4 of *Trp53* (3000 bps prior to ME- $\Delta 123p53$ starting codon) into the luciferase reporter plasmid. Promoter mapping was carried out by sequential deletion (Fig. 3c). The results from the luciferase assay revealed that two regions (–1000 to –500 and –2500 to –2000 bps prior to transcript starting site) appeared to be responsible for LDA-induced luciferase signal (Fig. 3c, d). These two regions were similarly responsive to LDR and VK_3 treatment (Fig S3E), which was further verified by deletion of each sequence, individually (Fig. 3e). Consistent with HIF1-mediated ME- $\Delta 123p53$ induction, knockdown of the expression of HIF1 α brought luciferase signal back to the basal level (Fig. 3f).

It was shown previously that $\Delta 133p53$ was transcriptionally regulated by p53 [4]. We further verified the finding by using MEFs isolated from $p53^{\text{R172H}}$ mice. The results showed that wild-type p53 was necessary for inducing the protective effect of ME- $\Delta 123p53$ (Fig S3F, G). Since the promoter sequences 1000–500 and 2500–2000 of ME- $\Delta 123p53$ were required for its induction, we searched these two regions for potential p53-binding site and indeed found p53 RE in each region. The binding of p53 to these sites was confirmed by ChIP-qPCR (Fig. 3g). Interestingly, HIF1 α was also required because its knockdown impeded p53 binding to these sites on ME- $\Delta 123p53$ promoter, suggesting a functional interaction between p53 and HIF1 in regulation of ME- $\Delta 123p53$ expression. Of note, the two confirmed p53 REs are shown bound by HIF1 α in a published ChIP-Seq dataset [12] (Fig S3H), consistent with a sequence homolog shared by p53RE and HRE [12].

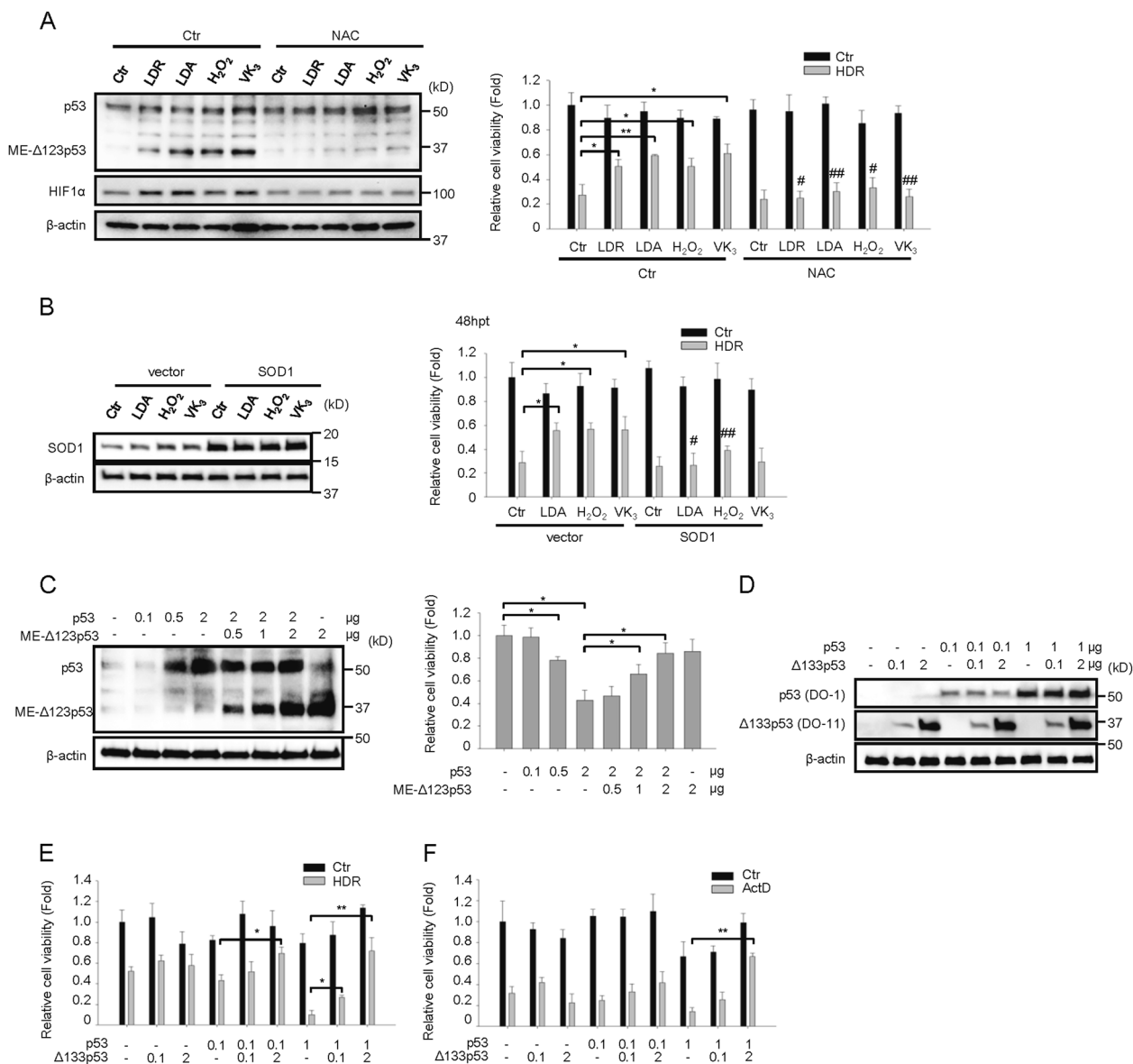


Fig. 2 Low level ROS-induced ME-Δ123p53 adjusts p53 signaling. **a** MEF cells were pretreated with 10 mM NAC for 4 h, and then treated with 0.1 Gy X-ray (LDR), LDA, 50 μM H₂O₂, or 0.5 μM VK₃. (Left) Protein level of p53, ME-Δ123p53, and HIF1α were measured. 12 h later, culture medium was changed and cells were subjected with HDR. (Right) 48hpt, relative cell viability was measured. **b** MEFs were transfected with plasmids expressing SOD1 or empty vector, and pretreated with LDA, 50 μM H₂O₂ or 0.5 μM VK₃ at 12 h post transfection. Then cells were subjected with HDR treatment. (Left) Protein level of SOD1 was checked before HDR. (Right) Cell viability was checked at 48 hpt. **c** MEFs were transfected with different ratio of p53 plasmids and ME-Δ123p53 plasmids as shown (completed with

empty vector). (Left) Protein level of SOD1 was checked. (Right) After 48h, relative cell viability was measured. **d** Human H1299 cells were transfected with different ratio of human p53 plasmids and Δ133p53 plasmids as shown (completed with empty vector). The transfection efficiency was checked by immunoblot. **e** Then cells were treated with HDR. Relative cell viability was measured at 48hpt. **f** Cells in **d** were treated with 5 nM ActD for 12 h. Relative cell viability was measured at 24hpt. Data are presented as mean ± standard deviation, **P* < 0.05, ***P* < 0.01, Anova test. For comparing with the corresponding control sample, “#” was used instead of “**” for indicating *P* value range

ME-Δ123p53 protects cells against acute stresses by suppression of apoptosis

We next explored the mechanism behind ME-Δ123p53-dependent protection. It was reported that Δ133p53/Δ113p53 could antagonize p53-dependent apoptosis [13–15]. We asked

if ME-Δ123p53 shared the same function by using the caspase inhibitor Z-VAD-FMK to assess LDA, low dose H₂O₂, or VK₃-induced protection. Interestingly, Z-VAD-FMK attenuated HDR-induced cell death only in vehicle treated cells but had minimum effect on LDA, H₂O₂, or VK₃-pretreated cells (Fig. 4a), implying that the protective effect is caused by

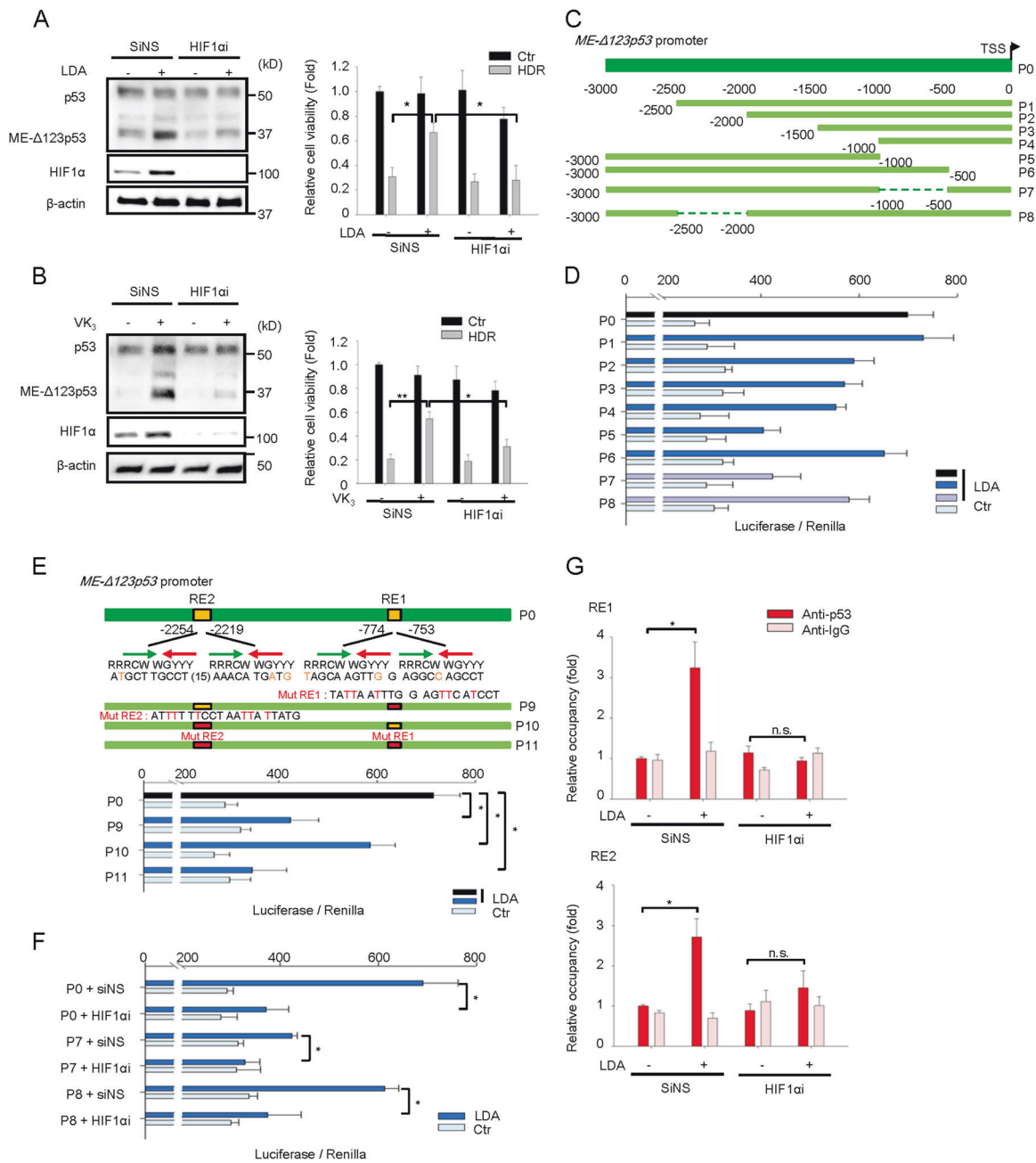


Fig. 3 ME- $\Delta 123p53$ induction is dependent on HIF pathway. **a** MEFs were transfected with HIF1 α siRNA (HIF1 α i) or siNS, then pretreated with LDA. (Left) Protein level of p53, ME- $\Delta 123p53$ and HIF1 α were measured. After 12 h, (right) MEFs were treated with HDR, and cell viability was measured at 48hpt. **b** MEFs were transfected with HIF1 α siRNA (HIF1 α i) or siNS, then pretreated with 0.5 μ M VK₃ for 12 h. (Left) Protein level of p53, ME- $\Delta 123p53$, and HIF1 α were measured. After 12 h, (right) MEFs were treated with HDR, and relative cell viability of MEFs was measured at 48hpt. **c** The 3000 bp sequence before ME- $\Delta 123p53$ start codon was cloned into pGL3 luciferase reporter backbone for ME- $\Delta 123p53$ promoter analysis. Then different parts of ME- $\Delta 123p53$ promoters were cloned to drive luciferase as shown. MEFs were transfected with luciferase reporters, and then treated with LDA. **d** Luciferase activity was checked at 12hpt, and normalized with co-transfected Renilla signal. **e** Two promoting response elements (RE) of p53 were predicted on -1000 to -500 and -2500 to -2000 regions of ME- $\Delta 123p53$ promoter. The green and red

arrows indicate the orientations of the quarter sites. The numbers in brackets indicate the distance (bps) between two half parts of binding motif. R = A or G, W = A or T, Y = C or T. The sequences of REs were shown in the diagram. Promoter with mutated p53-binding sites was cloned as luciferase reporter, and checked by luciferase assay. **f** MEFs were transfected with indicated luciferase reporters, combining with HIF1 α siRNA or nonsense siRNA, and treated with LDA. Luciferase signal was checked at 12hpt. **g** MEFs were transfected with HIF1 α or siNS, and treated with LDA. ChIP assay was performed with anti-p53-antibody (1C12) or anti-IgG antibody at 12hpt. Specific primer pairs were designed to amplify the corresponding REs. DNA was normalized with a pair of negative control primers for β -actin exon. The results are presented as the relative occupancies of different REs. Data are presented as mean \pm standard deviation, * P < 0.05, ** P < 0.01, Anova test. For comparing with the corresponding control sample, “#” was used instead of “**” for indicating P value range

increased resistance to apoptosis. In accordance, measurement of apoptotic cells revealed that HDR-induced apoptosis was significantly reduced by LDA-pretreatment but this effect of LDA was lost upon ME- Δ 123p53 knockdown (Fig. 4b, c), indicating that LDA-induced resistance was mediated by the antiapoptotic activity of ME- Δ 123p53.

We next investigated how ME- Δ 123p53 could enhance cellular resistance to apoptosis. We first tested whether this activity of ME- Δ 123p53 depended on the DNA binding by generating two ME- Δ 123p53 mutants R172H and R270H, corresponding to two hot mutation sites on human p53, R175H, and R282W, which are known to cause loss of DNA-binding capability of p53 [16]. When assessed in parallel with wild-type (WT) ME- Δ 123p53, both DNA-binding mutants were unable to protect cells against HDR (Fig. 4d), indicating that ME- Δ 123p53-mediated protection depends on its binding to DNA.

In light of the observations that LDA-induced resistance to apoptosis also depended on functional p53, we examined whether p53-regulated apoptotic genes might be involved. As expected, HDR-induced p53 activation was associated with induction of *Aif*, *Sco2*, *Mdm2*, *Bax*, *Cdkn1a*, *Puma*, and suppression of *Bcl2* (Figs. 4f, S4A, C). Interestingly, LDA-induced resistance to apoptosis was correlated with sustained levels of Bcl-2 (Fig. 4e, f). Using a complementary under- and overexpression approach, we demonstrated a ME- Δ 123p53-dependent expression of Bcl2 (Figs. 4f, S4A, B). A requirement of functional p53 in ME- Δ 123p53-mediated regulation of Bcl2 expression was validated with p53^{R172H} MEFs in which Bcl2 was not induced (Fig S4D).

A requirement of Bcl-2 for ME- Δ 123p53-mediated resistance was confirmed by Bcl-2 knocking down, which led to a failure of ME- Δ 123p53 to enhance cell survival (Fig. 4g). Together, our data showed that ME- Δ 123p53-induced resistance was mediated by Bcl2, in a mechanism dependent on p53.

ME- Δ 123p53/p53 form a complex and switch p53-binding sites on *Bcl2* promoter to promote *Bcl2* transcription

Our data aforementioned suggested a functional interaction between p53 and ME- Δ 123p53 in transcriptional regulation of Bcl2 expression. Of note is that ME- Δ 123p53 seemed to convert p53-mediated suppression into activation of Bcl2 expression. In light of the fact that p53 can either transcriptionally activate or suppress gene expression according to promoter sequences, we explored the possibility that the interaction between p53 and ME- Δ 123p53 might alter the DNA binding causing a shift from the repressing to activating sequence. Based on published p53/ Δ 133p53-binding consensus promoter sequences, we used a similar searching

algorithm recently published [5, 17] to perform an in silico analysis of *Bcl2* promoter sequences. The analysis uncovered five REs where R1, R2, and R3 are suppressive whereas R4 and R5 are activating (Fig. 5a). To test the contribution of each RE to p53/ME- Δ 123p53-mediated regulation of Bcl-2 expression, we cloned the 3000 bp promoter sequence prior to *Bcl2* transcription start site into a luciferase reporter vector with mutations of either activating REs (Mut1) or suppressive REs (Mut2) (Fig. 5b). These reporter vectors were then expressed in cells to assess the effect of p53 and ME- Δ 123p53 either individually or in combination. The result from the luciferase assay revealed that whereas p53 suppressed Bcl2 RE activity, as expected, ME- Δ 123p53 reversed p53-mediated inhibition. Mutation of the activating REs (Mut1) did not affect p53-mediated suppression but abrogated the effect of ME- Δ 123p53, whereas mutation of the suppressive REs (Mut2) was associated with a loss of p53-mediated inhibition (Fig. 5c). The data together suggest that upon expression, ME- Δ 123p53 switch the p53 binding from repressive REs to activating REs within the *Bcl2* promoter. The effect from expressed p53 and ME- Δ 123p53 on *Bcl2* promoter was reproduced by the LDA treatment, which recovered the luciferase activity in ActD-treated WT and Mut2 expressing MEFs but not Mut1 cells (Fig. 5d), suggesting that LDA-induced ME- Δ 123p53 switched p53 binding from repressive to activating REs.

To verify the binding data, we performed co-immunoprecipitation (CoIP) and ChIP with cells expressing HA-p53 and Myc-ME- Δ 123p53 separately or together (Fig. 5e, f). The CoIP result confirmed the association between p53 and ME- Δ 123p53. Quantification of each RE from the ChIP revealed that when expressed alone, p53 mainly bound to R1, R2, or R3, the suppressive REs, whereas when co-expressed with ME- Δ 123p53, there was little binding of R1, R2, or R3 but significant binding of R4 or R5 by ME- Δ 123p53 and p53. The data are consistent with the result from the luciferase assay that the expression of ME- Δ 123p53 shifts the p53 binding to *Bcl2* promoter from repressive to activating REs, resulting in restoration of Bcl2 expression.

ME- Δ 123p53 also upregulates glycolysis to protect cells from high-dose irradiation

We recently reported that ME- Δ 123p53 can regulate glycolysis via interaction with Δ Np63 [18]. We asked whether the ME- Δ 123p53/p53 interaction could similarly affect glycolysis and impact on cell survival. When cells expressing ME- Δ 123p53 were compared with the vector control, a number of glycolytic genes including *Hkl*, *Glut1*, and *Pgm* were significantly increased (Fig. 6a). In agreement with the elevated levels of glycolytic gene expression, the rate of glycolysis, not mitochondria respiration, was higher in ME-

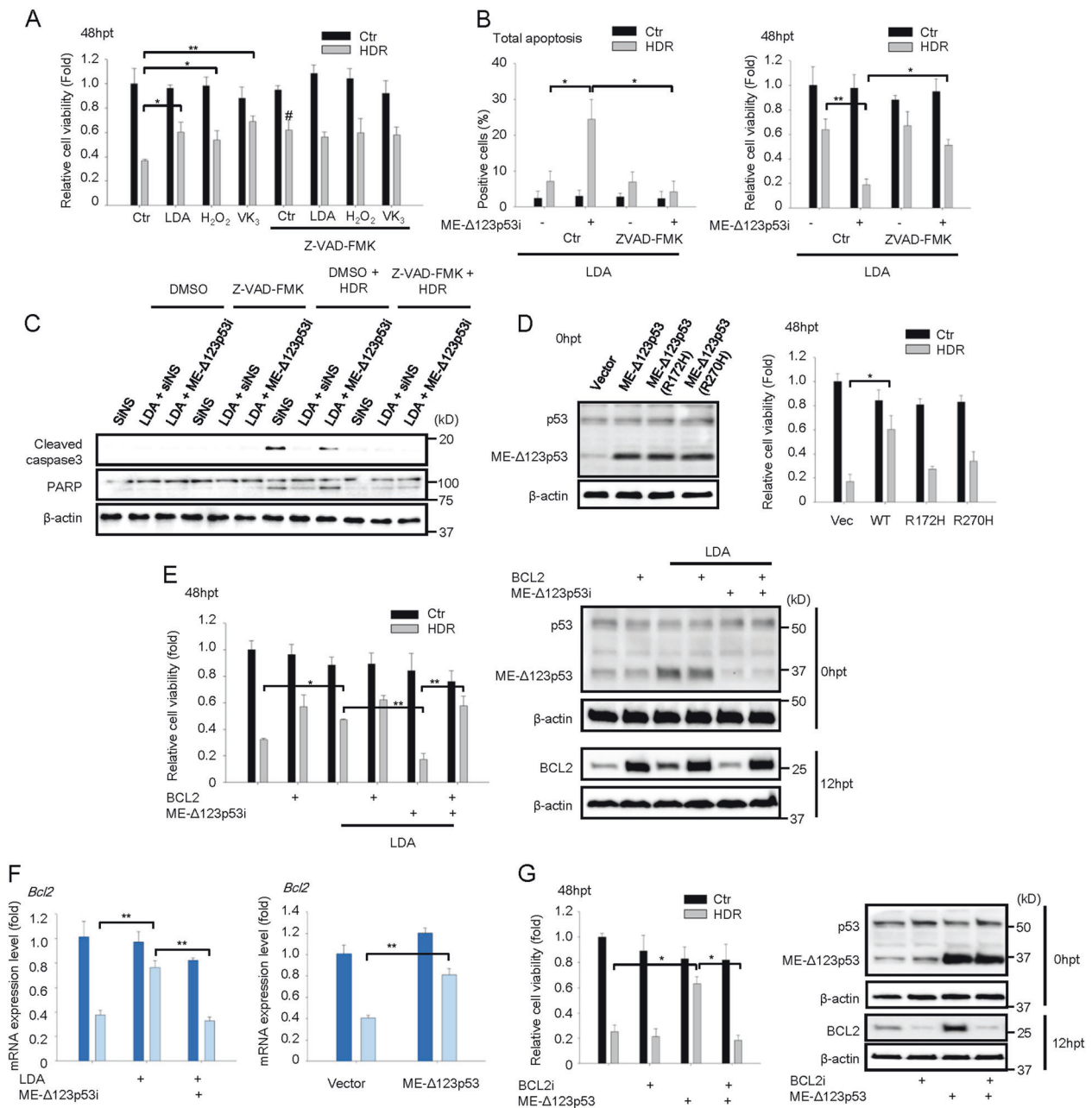
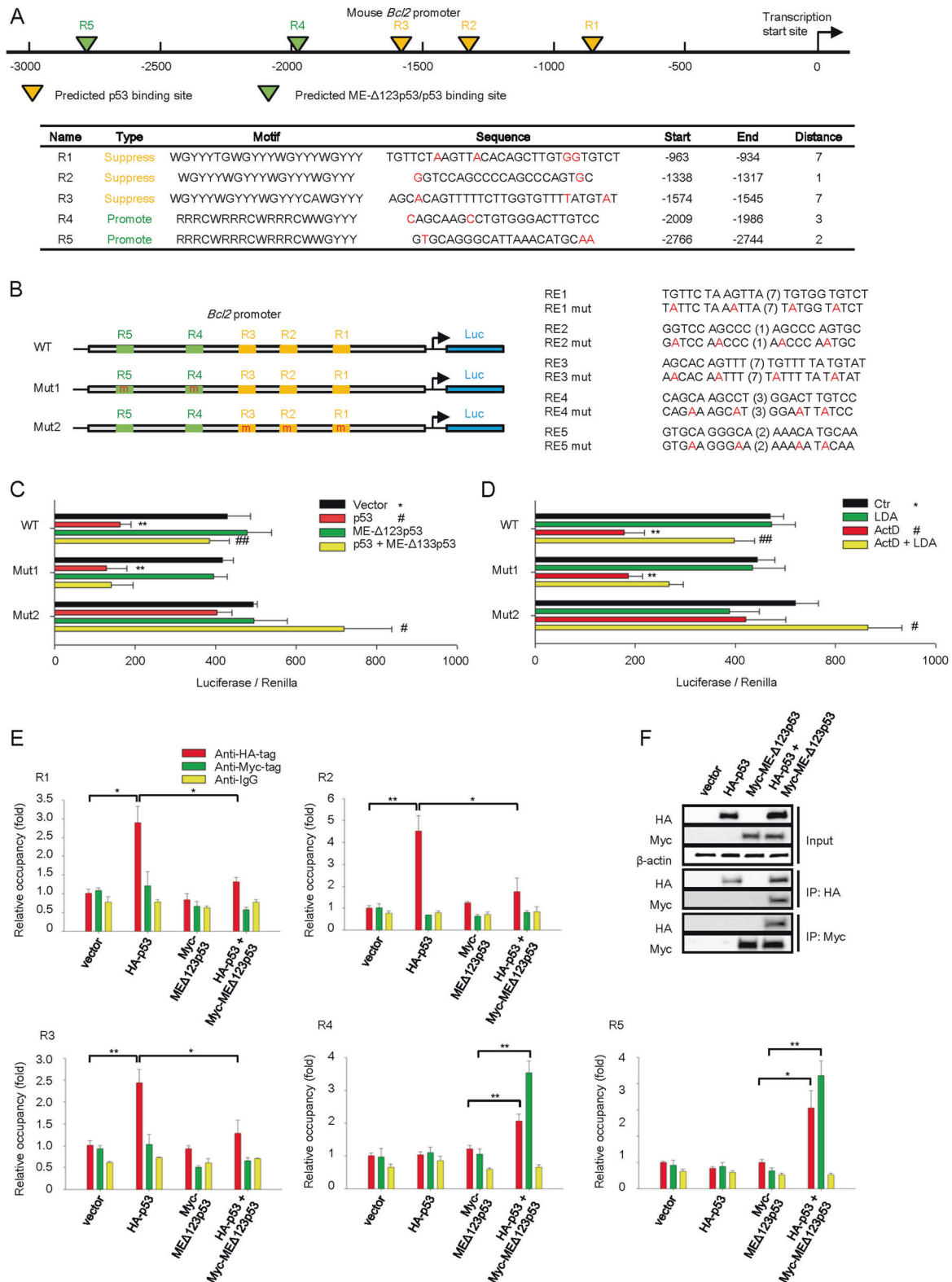


Fig. 4 ME- $\Delta 123p53$ suppresses apoptosis via switching p53 pathway to upregulate BCL2. **a** MEFs were pretreated with LDA, 50 μ M H₂O₂, or 0.5 μ M VK₃ for 12 h, and then treated with HDR. Caspase inhibitor 20 μ M Z-VAD-FMK was added in culture medium 30 min before irradiation. 48hpt, relative cell viability was measured as shown. **b** MEFs were transfected with ME- $\Delta 123p53i$ or siNS, then pretreated with LDA for 12 h. At 12 h post LDA treatment, combining with Z-VAD-FMK or not, cells were subjected with HDR. (Left) Total apoptosis cells ratio was determined by Annexin V/ 7-AAD dual staining—FACS assay. (Right) Relative cell viability was measured at 48hpt. **c** Cleaved caspase3 and PARP were measured by immunoblots. **d** MEFs were transfected with wild-type (WT) ME- $\Delta 123p53$, ME- $\Delta 123p53$ (R172H), or ME- $\Delta 123p53$ (R270H) mutation. (Left) Transfection efficiency was determined at 12 h post transfection. (Right) Then cells were treated with HDR, and cell viability was determined at 48hpt. **e** MEFs transfected with ME- $\Delta 123p53i$, BCL2

expressing plasmids or their combination (completed with siNS and empty vector) at 12 hpt as shown. **f** (Left) MEFs transfected with ME- $\Delta 123p53i$ or siNS were treated with LDA at 12 h post transfection. After 12 h, cells were treated with HDR. *Bcl2* mRNA level was measured by qRT-PCR at 12 hpt. (Right) MEFs transfected with ME- $\Delta 123p53$ or empty vector were treated with HDR at 12 h post transfection. After 12 h, *Bcl2* mRNA level was measured by qRT-PCR. **g** MEFs transfected with ME- $\Delta 123p53$ plasmid, BCL2i siRNA (Bcl2i) or their combination (completed with siNS and empty vector) were treated with HDR at 12 h post transfection. (Left) Relative cell viability was measured at 48hpt. (Right) Protein level of p53 and ME- $\Delta 123p53$ was measured before HDR treatment and protein level of BCL2 was measured at 12hpt as shown. Data are presented as mean \pm standard deviation, * P < 0.05, ** P < 0.01, Anova test. For comparing with the corresponding control sample, “#” was used instead of “*” for indicating P value range



Δ123p53 expressing cells than controls (Fig. 6b). Enhanced glycolytic metabolism can promote survival, [19–21] which may contribute to the protective function of ME-Δ123p53. We tested this by inhibition of glycolysis with 2-deoxy-D-

glucose (2-DG). Interestingly, 2-DG impeded the anti-apoptotic effect of ME-Δ123p53 at early time point (8 h post HDR), but this effect was diminished later (12 h post HDR) (Fig. 6c). Consistently, treatment with 2-DG slightly

Fig. 5 The ME- $\Delta 123p53/p53$ complex directly binds to different sites of the *Bcl2* promoter than p53 alone, enabling the fine regulation of *Bcl2* transcription. **a** Diagram shows the 3000 bps of mouse *Bcl2* promoter and in silico predicted p53 family members binding sites on it. The sequences and positions of p53 family REs on *Bcl2* promoter are listed below. R = A or G, W = A or T, Y = C or T, here the red font indicates bases not perfectly match the motif pattern. **b** The 3000 bps of mouse *Bcl2* promoter was cloned in luciferase backbone as the WT promoter reporter control. The REs on *Bcl2* promoter were mutated for investigating their function. The WT and mutated REs sequences were listed as the diagram shown. **c** Reporter plasmids with WT or mutant *Bcl2* promoter were transfected in MEFs pre-transfected with p53, ME- $\Delta 123p53$ or their combination. **d** Reporter plasmids were transfected in MEFs pretreated with LDA, pre-transfected with ME- $\Delta 123p53$ or the combination treatment. The luciferase activity was measured. Reporter luciferase signals were normalized with co-transfected Rellina signals. **e** ChIP of p53/ME- $\Delta 123p53$ specific REs (response elements) in *Bcl2* promoters in MEF cells at 12 h post transfected with HA tagged p53, myc tagged ME- $\Delta 123p53$ or their combination. Anti-HA-tag or Anti-myc-tag antibody was used to co-immunoprecipitate the protein-DNA complex, while IgG was used as a non-specific binding control. Specific primer pairs were designed to amplify the corresponding REs. DNA was normalized with a pair of negative control primers for β -actin exon. The results are presented as the relative occupancies of different REs. **f** CoIP with Anti-HA-tag or Anti-myc-tag antibody in MEF cells transfected with HA-p53, myc-ME- $\Delta 123p53$ or their combination as indicated. Data are presented as mean \pm standard deviation, * $P < 0.05$, ** $P < 0.01$, Anova test. For comparing with the corresponding control sample, “#” was used instead of “*” for indicating P value range

attenuated ME- $\Delta 123p53$'s protective effect on cell viability (Fig. 6d). The data suggest that apart from regulation of *Bcl2* expression, ME- $\Delta 123p53$ also induced glycolysis that contributed, albeit to a modest level, to cell survival. We corroborated the results derived from ME- $\Delta 123p53$ expression with LDA and LDR treated cells (Fig S5A–D).

ME- $\Delta 123p53/p53$ -mediated protection of tissue injury induced by high-dose radiation in vivo

To test the biological relevance of ME- $\Delta 123p53$ -mediated protection, we extended our study in vivo. C57BL mice were treated with LDA or LDR for 5 consecutive days then subjected to HDR as depicted (Fig S6A). LDA and LDR pretreated mice survived significantly longer than the control group (Fig. 7a). LDA could also extend survival time in ActD-treated mice (Fig. 7b). Immunoblot analysis of tissue extracts revealed that LDA or LDR treatment induced the expression of ME- $\Delta 123p53$ in the spleen, thymus, duodenum, pancreas, liver, lung, and kidney relative to the control group (Fig S6B, C). Both LDA and LDR-induced protection were associated with reduced apoptotic response to HDR, as indicated by the TUNEL staining (Fig. 7c) and western detection of cleaved Caspase3 (Fig S6D, E). Of note, the protection was more apparent in the sensitive tissues such as the spleen, thymus, duodenum, and pancreas, whereas the less sensitive tissues for instance the liver, lung and kidney were

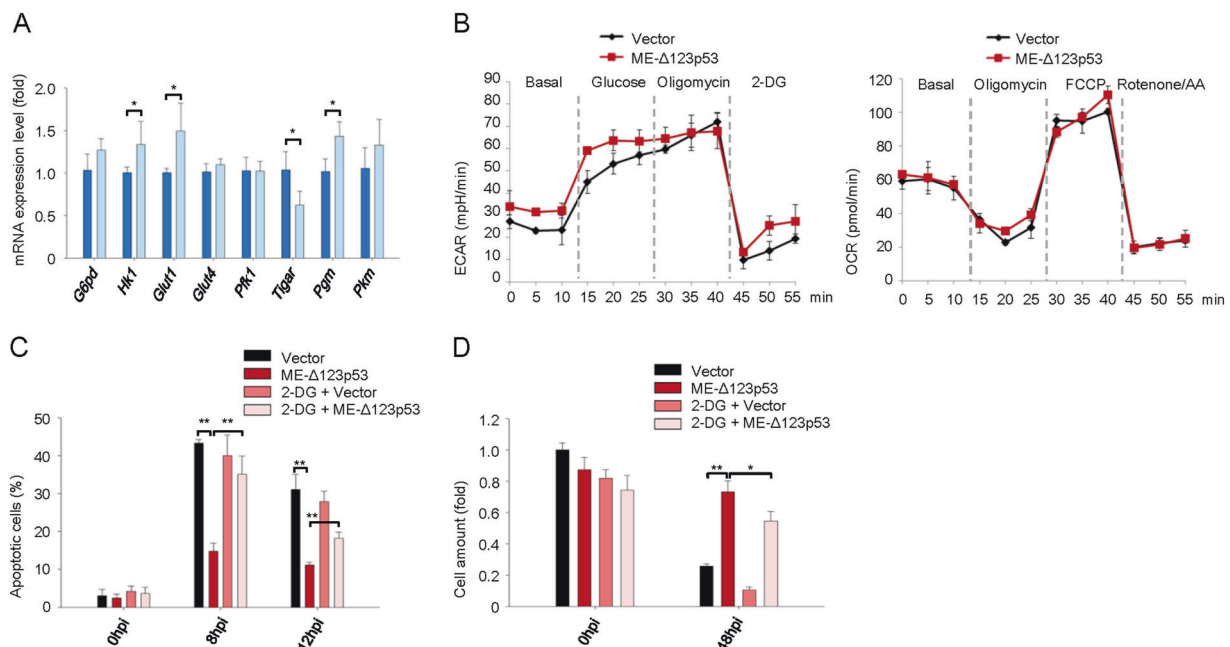
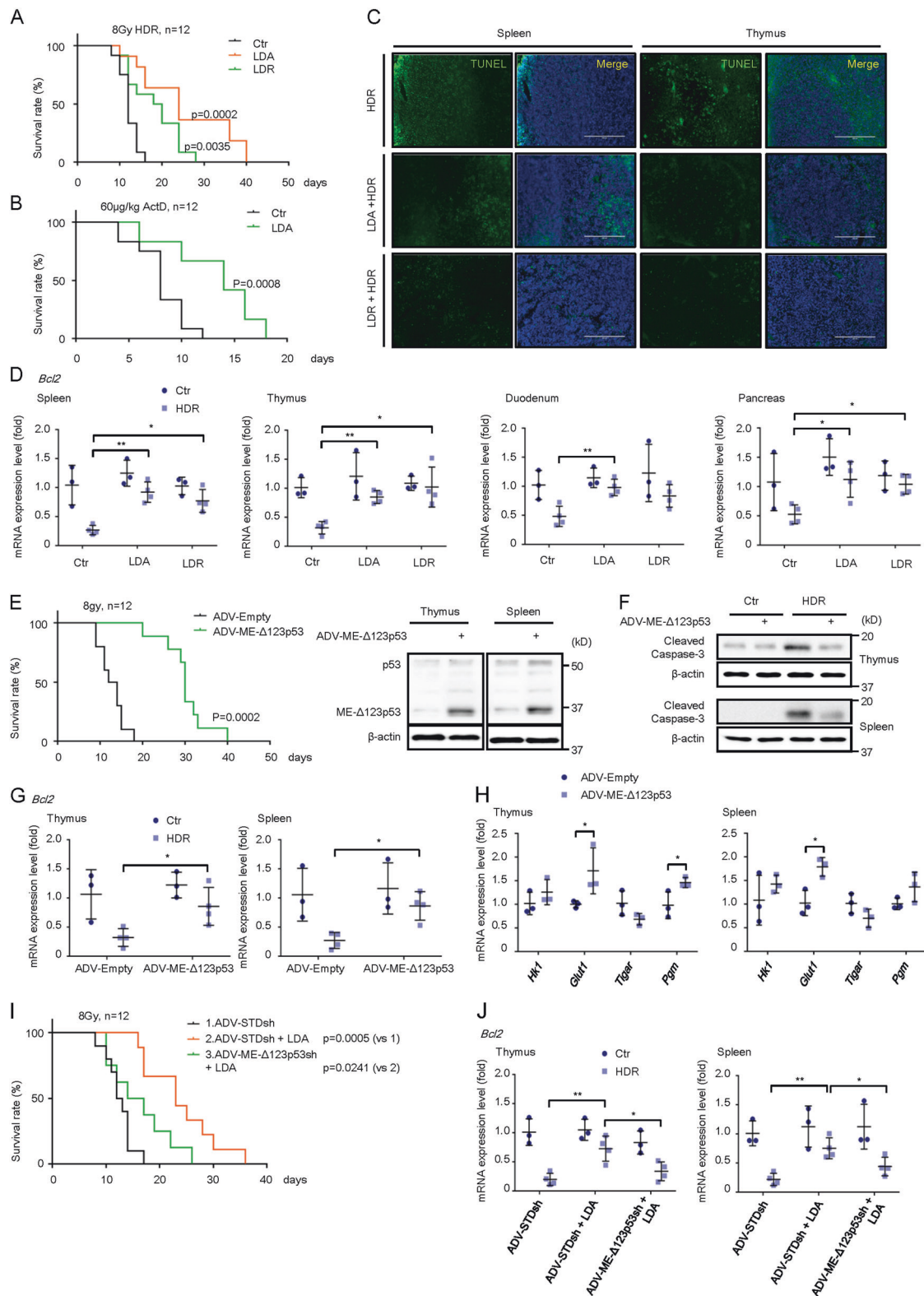


Fig. 6 ME- $\Delta 123p53$ moderately promotes glycolysis to suppress apoptosis at early stage. **a** MEFs were transfected with ME- $\Delta 123p53$ or empty vector at 12 h post transfection. Glycolytic genes mRNA level were checked with qRT-PCR, Extracellular acidification rate (ECAR) and **b** mitochondria oxygen consumption rate (OCR) were measured with seahorse assay at 12 h post transfection. **c** Cells in

a were subjected to HDR, and total apoptosis cells ratio was determined by Annexin V/ 7-AAD dual staining—FACS assay at 0 h, 8 h, and 12hpi. **d** Cell viability was measured at 0 h and 48hpi. Data are presented as mean \pm standard deviation, * $P < 0.05$, ** $P < 0.01$, Anova test



not as responsive. In line with the diminished apoptosis in LDR and LDA-pretreated animals, HDR-induced *Bcl2* downregulation was significantly attenuated (Figs. 7d, S6F). The association of LDA or LDR-induced protection with

increased expression of ME- Δ 123p53 implicates a role for this p53 isoform in the induced resistance. To confirm this, we overexpressed ME- Δ 123p53 via adenoviral-mediated gene transfer in mice. Relative to the empty vector control,

◀ **Fig. 7** Moderate stimulation induced ME- $\Delta 123p53$ protects multiple organs from acute stress in vivo. **a** C57BL mice ($n = 12$ per group) were treated with 0.1 Gy X-ray (LDR, once per day) or low dose arsenic (LDA, IP with 0.4 mg/kg arsenic) for 5 consecutive days, and then subjected with 8 Gy X-ray. **b** Mice ($n = 12$ per group) were injected with LDA for 5 consecutive days, and subjected to low dose ActD treatment (IP with 60 $\mu\text{g}/\text{kg}$ ActD, once per day). Survival rate was recorded and plotted as indicated. **c** Mice were treated with LDR or LDA as in **a** and then subjected with 4 Gy X-ray. Mice were sacrificed and indicated organs were collected at 12hpi. TUNEL assay was performed with slices of spleen and thymus as shown. **d** In thymus, spleen, duodenum, and pancreas, *Bcl2* mRNA expression level was measured by qRT-PCR. **e** Mice ($n = 12$ per group) were injected with empty adenovirus (ADV-Empty) or adenovirus expressing ME- $\Delta 123p53$ (ADV-ME- $\Delta 123p53$) (IP with 6×10^9 pfu adenovirus). Five days later, mice were subjected to 8 Gy X-ray irradiation. (Left) Survival rate was recorded and plotted as indicated. (Right) Mice were injected with indicated agents, and then subjected with 4 Gy X-ray. Mice were sacrificed and indicated organs were collected at 12hpi. Protein level of p53, ME- $\Delta 123p53$ and **f** Cleaved-caspase3 was measured. **g** *Bcl2* and **h** indicated glycolytic genes mRNA expression level was measured by qRT-PCR. **i** Mice ($n = 12$ per group) were injected with adenovirus expressing nonsense shRNA (ADV-STDsh) or shRNA targeting ME- $\Delta 123p53$ (ADV-ME- $\Delta 123p53\text{sh}$), and then injected with LDA for 5 consecutive days. Next day, mice were subjected with 8 Gy X-ray. Survival rate was recorded and plotted as indicated. **j** Mice were injected with indicated agents as in **i**, but then subjected with 4 Gy X-ray. Mice were sacrificed and indicated organs were collected at 12hpi. *Bcl2* mRNA expression level was measured by qRT-PCR. Data are presented as mean \pm standard deviation, * $P < 0.05$, ** $P < 0.01$, Anova test

mice with ME- $\Delta 123p53$ overexpression had a significantly increased survival following 8 Gy irradiation. Associated with the survival were less caspase activation (Fig. 7e, f) and diminished reduction in *Bcl2* expression (Fig. 7g). Interestingly, glycolytic genes were also elevated in ME- $\Delta 123p53$ expressing mice (Fig. 7h). To complement the overexpression experiment, we reduced the expression of ME- $\Delta 123p53$ via adenoviral expression of ME- $\Delta 123p53\text{sh}$, which was associated with significantly enhanced sensitivity to HDR (Figs. 7i, j, S7G, H). The data collectively demonstrate that LDA and LDR-induced resistance in mice are mediated by ME- $\Delta 123p53$.

Discussion

As a protein extremely responsive to stress, p53 can mediate the prodeath response to severe stress and is also implicated in mild stress-induced adaptive protection [1, 11, 21]. This p53-mediated adaptive prosurvival activity represents an apparent departure from its canonical prodeath function. We demonstrate that through the interaction with $\Delta 133p53$ (ME- $\Delta 123p53$ in mice), the proapoptotic function of p53 can be switched to antiapoptotic, dependent on the relative abundance of ME- $\Delta 123p53/\Delta 133p53$ versus p53. The expression of ME- $\Delta 123p53/\Delta 133p53$ is preferentially induced by low levels of stress, which have little effect on p53. Unlike p53,

ME- $\Delta 123p53/\Delta 133p53$ has a much longer half-life and is able to be accumulated due to lacking of MDM2-binding sites [13]. As a consequence, the ratio of ME- $\Delta 123p53(\Delta 133p53)/p53$ rises resulting in enhanced cell survival upon subsequent acute stress. In the context of stress adaptive response, p53 is not strongly induced because of less DNA damage. In response to severe or harsh stress, however, p53, but not ME- $\Delta 123p53/\Delta 133p53$, is dominantly induced leading to p53-dependent cell death.

The prosurvival function of $\Delta 133p53$ has been reported, though its underlying mechanism is only beginning to be elucidated [2, 5, 14, 17, 18, 22–26]. Because of lacking the TAD, $\Delta 133p53$ does not have any intrinsic transcription activity. However, $\Delta 133p53$ has been shown to interact with and modulate p53 transcription activity [2, 4, 22]. We show that ME- $\Delta 123p53$ can shift p53-mediated binding to the *Bcl2* promoter from repressive to activating REs (similar REs were also found in human *BCL2* promoter as shown in Fig S7A). The ME- $\Delta 123p53$'s DBD is almost identical to that of p53 except missing the N-terminal 36 amino acid residues. Interestingly, addition of the 36aa to ME- $\Delta 123p53$ DBD abrogated the binding to activating REs (Fig S7B–D), implicating a unique structure of ME- $\Delta 123p53/\Delta 133p53$ DBD critical in activating RE binding. Further structural analysis would be necessary to address this issue.

The ME- $\Delta 123p53/\Delta 133p53$ -dependent prosurvival induced by low levels of stress represents a novel mechanism underlying the widely observed phenomenon, hormesis, i.e., mild stress induces cellular resistance to subsequent exposure to harsh stress. In line with an effect that was specific to mild stress, increased ME- $\Delta 123p53/\Delta 133p53$ expression was mediated via elevated ROS induced by the treatment with subtoxic levels of chemicals. (A similar observation was made with human fibroblasts in Fig S8). In this context, HIF1, an ROS-responsive protein, was induced and contributed to the upregulation of ME- $\Delta 123p53/\Delta 133p53$ expression. Of interest is that ME- $\Delta 123p53/\Delta 133p53$ expression also depends on wild-type p53. While it is presently unclear how HIF1 and p53 may interact with each other in regulation of ME- $\Delta 123p53/\Delta 133p53$, a high degree of homology within the REs of HIF1 and p53 suggests a coordinated regulation. Further study is necessary to dissect p53/HIF1-mediated ME- $\Delta 123p53/\Delta 133p53$ regulation.

Apart from the regulation of *Bcl2* expression, $\Delta 133p53$ likely contributes to cell survival through additional mechanisms [3, 5, 17, 18]. In accordance with this notion, this p53 isoform appears to enhance cell survival by promoting glycolysis. While multiple pathways might be integrated to determine cell survival or death, our data indicates that ME- $\Delta 123p53/\Delta 133p53$ -mediated regulation of *Bcl2* expression seems to be the dominant mechanism

behind the prosurvival function of ME- Δ 123p53/ Δ 133p53 in the context of stress adaptive response.

Data availability

The authors declare that the main data supporting the findings of this study are within the article and its Supplementary Information files. Extra data are obtained from the corresponding authors upon request.

Acknowledgements This work was supported in part by the Morningside Foundation, the Zhu Fund and grants from the National Cancer Institute at the National Institutes of Health (R01CA233558, R01CA167814, and R01CA125144).

Compliance with ethical standards

Conflict of interest The authors declare that they have no conflict of interest.

Publisher's note Springer Nature remains neutral with regard to jurisdictional claims in published maps and institutional affiliations.

References

- Kruiswijk F, Labuschagne CF, Vousden KH. p53 in survival, death and metabolic health: a lifeguard with a licence to kill. *Nat Rev Mol cell Biol*. 2015;16:393–405.
- Chen J, Ruan H, Ng SM, Gao C, Soo HM, Wu W, et al. Loss of function of def selectively up-regulates Delta113p53 expression to arrest expansion growth of digestive organs in zebrafish. *Genes Dev*. 2005;19:2900–11.
- Jorujiz SM, Bourdon JC. p53 Isoforms: key regulators of the cell fate decision. *Cold Spring Harb Perspect Med*. 2016;6:a026039.
- Marcel V, Vijayakumar V, Fernandez-Cuesta L, Hafsi H, Sagne C, Hautefeuille A, et al. p53 regulates the transcription of its Delta133p53 isoform through specific response elements contained within the TP53 P2 internal promoter. *Oncogene*. 2010;29:2691–2700.
- Gong L, Gong H, Pan X, Chang C, Ou Z, Ye S, et al. p53 isoform Delta113p53/Delta133p53 promotes DNA double-strand break repair to protect cell from death and senescence in response to DNA damage. *Cell Res*. 2015;25:351–69.
- Lionnet T, Czaplinski K, Darzacq X, Shav-Tal Y, Wells AL, Chao JA, et al. A transgenic mouse for in vivo detection of endogenous labeled mRNA. *Nat methods*. 2011;8:165–70.
- He TC, Zhou S, da Costa LT, Yu J, Kinzler KW, Vogelstein B. A simplified system for generating recombinant adenoviruses. *Proc Natl Acad Sci USA*. 1998;95:2509–14.
- Purbey PK, Scumpia PO, Kim PJ, Tong AJ, Iwamoto KS, McBride WH, et al. Defined sensing mechanisms and signaling pathways contribute to the global inflammatory gene expression output elicited by ionizing radiation. *Immunity*. 2017;47:421–34 e423.
- Roth I, Campbell H, Rubio C, Vennin C, Wilson M, Wiles A, et al. The delta133p53 isoform and its mouse analogue delta122p53 promote invasion and metastasis involving pro-inflammatory molecules interleukin-6 and CCL2. *Oncogene*. 2016;35:4981–9.
- Slatter TL, Hung N, Campbell H, Rubio C, Mehta R, Renshaw P, et al. Hyperproliferation, cancer, and inflammation in mice expressing a delta133p53-like isoform. *Blood*. 2011;117:5166–77.
- Ganapathy S, Xiao S, Yang M, Qi M, Choi DE, Ha CS, et al. A low-dose arsenic-induced p53 protein-mediated metabolic mechanism of radiotherapy protection. *J Biol Chem*. 2014;289:5340–7.
- Guimaraes-Camboa N, Stowe J, Aneas I, Sakabe N, Cattaneo P, Henderson L, et al. HIF1alpha represses cell stress pathways to allow proliferation of hypoxic fetal cardiomyocytes. *Developmental Cell*. 2015;33:507–21.
- Aoubala M, Murray-Zmijewski F, Khoury MP, Fernandes K, Perrier S, Bernard H, et al. p53 directly transactivates delta133-p53alpha, regulating cell fate outcome in response to DNA damage. *Cell Death Differ*. 2011;18:248–58.
- Chen J, Ng SM, Chang C, Zhang Z, Bourdon JC, Lane DP, et al. p53 isoform delta113p53 is a p53 target gene that antagonizes p53 apoptotic activity via BclxL activation in zebrafish. *Genes Dev*. 2009;23:278–90.
- Gong L, Pan X, Chen H, Rao L, Zeng Y, Hang H, et al. p53 isoform Delta133p53 promotes efficiency of induced pluripotent stem cells and ensures genomic integrity during reprogramming. *Sci Rep*. 2016;6:37281.
- Bykov VJ, Issaeva N, Shilov A, Hultcrantz M, Pugacheva E, Chumakov P, et al. Restoration of the tumor suppressor function to mutant p53 by a low-molecular-weight compound. *Nat Med*. 2002;8:282–8.
- Gong L, Pan X, Yuan ZM, Peng J, Chen J. p53 coordinates with delta133p53 isoform to promote cell survival under low-level oxidative stress. *J Mol cell Biol*. 2016;8:88–90.
- Gong L, Pan X, Lim CB, de Polo A, Little JB, Yuan ZM. A functional interplay between delta133p53 and deltaNp63 in promoting glycolytic metabolism to fuel cancer cell proliferation. *Oncogene*. 2018;37:2150–64.
- Koppenol WH, Bounds PL, Dang CV. Otto Warburg's contributions to current concepts of cancer metabolism. *Nat Rev Cancer*. 2011;11:325–37.
- Lunt SY, Vander Heiden MG. Aerobic glycolysis: meeting the metabolic requirements of cell proliferation. *Annu Rev Cell Developmental Biol*. 2011;27:441–64.
- Lall R, Ganapathy S, Yang M, Xiao S, Xu T, Su H, et al. Low-dose radiation exposure induces a HIF-1-mediated adaptive and protective metabolic response. *Cell Death Differ*. 2014;21:836–44.
- Bourdon JC, Fernandes K, Murray-Zmijewski F, Liu G, Diot A, Xirodimas DP, et al. p53 isoforms can regulate p53 transcriptional activity. *Genes Dev*. 2005;19:2122–37.
- Rohaly G, Chemnitz J, Dehde S, Nunez AM, Heukeshoven J, Deppert W, et al. A novel human p53 isoform is an essential element of the ATR-intra-S phase checkpoint. *Cell*. 2005;122:21–32.
- Arsic N, Gadea G, Lagerqvist EL, Busson M, Cahuzac N, Brock C, et al. The p53 isoform delta133p53beta promotes cancer stem cell potential. *Stem Cell Rep*. 2015;4:531–40.
- Bernard H, Garmy-Susini B, Ainaoui N, Van Den Berghe L, Peurichard A, Javerzat S, et al. The p53 isoform, delta133p53alpha, stimulates angiogenesis and tumour progression. *Oncogene*. 2013;32:2150–60.
- Gong L, Chen J. Delta113p53/Delta133p53 converts P53 from a repressor to a promoter of DNA double-strand break repair. *Mol Cell Oncol*. 2016;3:e1033587.